Feasibility and Tailoring of Bioactive Glass-ceramic Scaffolds with Gradient of Porosity for Bone Grafting

(Article begins on next page)

03 May 2024

Feasibility and Tailoring of Bioactive Glass-ceramic Scaffolds

with Gradient of Porosity for Bone Grafting

CHIARA VITALE-BROVARONE∗, FRANCESCO BAINO AND ENRICA VERNÉ

Materials Science and Chemical Engineering Department, Politecnico di Torino,

Corso Duca degli Abruzzi 24, 10129, Italy

∗ Corresponding author: Chiara Vitale-Brovarone

E-mail: chiara.vitale@polito.it

Phone: +39 011 564 4716

Fax: +39 011 564 4699

ABSTRACT: The aim of this research work is the preparation and characterization of graded glass-ceramic scaffolds able to mimic the structure of the natural bone tissue, formed by cortical and cancellous bone. The material chosen for the scaffolds preparation is a glass belonging to the system SiO_2-P_2O_5-CaO-MgO-Na_2O-K_2O (CEL2). The glass was synthesized by a conventional melting-quenching route, ground and sieved to obtain powders of specific size. The scaffolds were fabricated by using different methods: polyethylene burn-off, sponge replication, a glazing-like technique and combinations of these methods. The scaffolds were characterized through morphological observations, density measurements, volumetric shrinkage, mechanical tests and *in vitro* bioactivity tests. The features of the scaffolds prepared with the different methods were compared in terms of morphological structure, pores content and mechanical strength.

The proposed scaffolds effectively mimic the cancellous/cortical bone system in terms of structure, porosity and mechanical strength and they exhibit a highly bioactive behaviour. Therefore, these graded grafts have a great potential for biomedical applications and can be successfully proposed for the substitution of load-bearing bone portions.

KEY WORDS: glass-ceramic, graded scaffold, bone tissue mimicking, bone grafting, porous bioceramic.

INTRODUCTION

Bone is a connective tissue characterized by high hardness and excellent mechanical properties. Bone cells are encased in a strong composite structure formed by collagen fibres, hydroxyapatite crystals, *i.e.* the reinforcing phase of the material and bone extracellular matrix. From a structural point of view, two main types of bone can be distinguished: (i) cortical bone and (ii) cancellous bone. The cortical bone is a continuous, dense bulk and occurs in the central part of the long bones, such as tibia or femur [1]. The cancellous bone, that is like a honeycomb in cross-section, occurs in the flat bones and across the ends of the long bones, that are covered by a thin coating of cortical bone such as a compact "skin" [2]. The ordered trabecular structure in the cancellous bone has maximum strength and toughness along the lines of the applied stresses [3]. It is difficult to evaluate a standard reference for bone strength because its mechanical properties depend on many parameters, such as harvest site, patient age and health, test sample preparation and test conditions. It was assessed and it is generally accepted a strength range of 2-12 MPa for cancellous bone, whereas for cortical bone a strength up to 200 MPa was found [4].

The presence and the amount of cortical and cancellous bone in the different bone segments of human body are closely related to the function that the bone itself should accomplish [5]. Due to the complexity of bone tissue microarchitecture and organization, the substitution of large bone portions, also located in load-bearing bone segments, is one of the most relevant challenges in orthopaedic surgery. Bone losses, due to trauma, tumours or other pathologies, were traditionally replaced by using autografts or allografts, but these implants have some drawbacks [6]. Autografts represent the "standard optimum" for bone substitutions, but problems of bone graft availability and risks of pain and/or morbidity in the harvest site can occur [7]. Allografts overcome the harvest drawbacks for the patient but can cause pathogen disease transfer from the donor to the patient, and problems concerning the graft quality can occur [8]. A promising solution that get over these disadvantages is the development of bioactive porous scaffolds in alloplastic materials able to

promote the growth of newly formed bone tissue and to maintain satisfactory mechanical properties to sustain the bio-mechanic load during the bone regeneration process [9].

The need to fabricate biocompatible scaffolds with mechanical strength comparable to human bone has attracted the interest of many researchers towards bioceramics. Hydroxyapatite (HA) has been traditionally used for hard tissue repair because of its chemical and crystallographic similarity to the carbonated apatite in human teeth and bone [10]. Calcium phosphate salts, such as β-tricalcium phosphate (β-TCP) can act as HA precursors and have usually been adopted as fillers for small bone cavities or in dentistry [11-12]. HA and β-TCP scaffolds exhibit an excellent biocompatibility but are characterized by poor mechanical strength (below 2 MPa) [13-14]. Bioactive glasses (BGs) and glass-ceramics (BGCs), basically composed of SiO_2, P_2O_5, Na_2O, CaO and produced via traditional melt-quench method or via sol-gel technique, have been investigated due to their tuneable bioactive behaviour [15-16]. BGs and BGCs have found extensive applications as orthopaedic and dental graft materials and, more recently, also for tissue engineering scaffolding [17-21]. Scaffolds for bone regeneration should have a 3-D structure similar to natural bone, with a highly interconnected pores network (pores content above 50 %vol.) [22]. Specifically, a scaffold must exhibit a bimodal distribution of porosity, formed by macropores (100-500 μm) and micropores (10-50 μm) [23]. Macroporosity allows bone cells to colonize the inner part of the implant and provides a 3-D network for blood vessels access [24]. Microporosity promotes proteins and cells attachment on the implant as it was demonstrated that cells spread preferably on a rough surface [25].

Bone tissue engineering scaffolds possessing the above mentioned requirements can be successfully produced from glass powders that undergo a sintering thermal treatment. The porosity can be introduced in the scaffold by using a thermally removable phase, such as polyethylene (PE) [18] or starch particles [26-27], or via a polymeric template (polyurethane sponge) [19], that burns-off during the sintering process.

This research work is focused on the feasibility of graded scaffolds by using different "state-of-art" methods of preparation and a bioactive glass (CEL2) as scaffold material [19,20]; porous implants

simulating the bimodal structure of bone (cancellous and cortical) were prepared in literature by using only HA and/or β-TCP [28-29]. Specifically, the methods reported in literature to produce graded structure use the replication method and involve the use of polyurethane (PU) sponge of different porosity [29] or multiple impregnation of a single PU sponge [28]. The PE burn-off method, the sponge replication and the glazing technique were adopted to fabricate bioactive glass-ceramic scaffolds with tailored gradients of porosity, able to effectively mimic both the natural structure of cancellous bone and the system cortical/trabecular bone.

MATERIALS AND METHODS

Materials

The chosen SiO_2-based glass belongs to the system SiO_2-P_2O_5-CaO-MgO-Na_2O-K_2O (CEL2) and has the following molar composition: 45% SiO_2, 3% P_2O_5, 26% CaO, 7% MgO, 15% Na_2O, 4% K_2O [19-20]. CEL2 was prepared by a traditional melting-quenching route: the raw products (SiO_2, $Ca_3(PO_4)_2$, $CaCO_3$, $(MgCO_3)_4 \cdot Mg(OH)_2 \cdot 5H_2O$, Na_2CO_3, K_2CO_3) were molten in a platinum crucible at 1400 °C for 1 h in air (heating rate set at 10 °C·min^{-1}) and the melt was then quenched in cold water to obtain a frit that was subsequently ground by balls milling and sieved to the desired size range.

A commercial open-cells polyurethane (PU) sponge ($\rho \approx 20$ kg·m^{-3}), characterized by a 3-D network of macropores, was used as sacrificial template for the replication method. Polyethylene particles (Wrigley Fibres, Somerset, UK) ranging within 300-600 μm were used for the PE burn-off technique.

Scaffolds preparation

In this work, different methods of preparation were tested to fabricate glass-ceramic scaffolds with gradients of porosity.

The features of the proposed methods, labelled as A-F, are resumed as follows:

Method A: the aim was to obtain scaffolds with a double porous layer; the samples were produced via PE burn-off technique. CEL2 powders, sieved below 106 μm, and PE particles were mixed together for 0.5 h in a polyethylene bottle by using a rolls shaker. Compacts of powders ("greens") were obtained in form of bars via stacking the mixed powders and uniaxially pressing them at 127 MPa for 10 s; the pressing conditions were optimized to obtain a crack-free material. Various amounts of PE particles were used to obtain samples with layers of different porosity. The green bodies were then thermally treated to remove the organic phase and to sinter the glass powders. Finally the samples were cut into blocks by using an adjustable speed diamond saw to obtain cubic scaffolds.

Method B: the aim was to obtain scaffolds coupling a porous structure with a compact one. The porous part was produced via PE burn-off (preparation conditions analogous to method A), whereas a glazing-like technique was used to realize the compact external layer. Specifically, a suspension of CEL2 powders in ethanol was prepared and applied on the scaffold surface with controlled deposition of powders for 24 h due to gravity.

Method C: scaffolds with a double-layer porous structure were produced via the sponge replication technique: the PU sponge was cut into blocks and then impregnated with a water based CEL2 slurry. The slurry was prepared by dispersing the glass powders into distilled water with polyvinyl alcohol (PVA) used as binder for the glass particles (weight ratio: 30% CEL2, 6% PVA, 64% water). First PVA was hydrolyzed and stirred at 60 °C for 1 h using a magnetic stirrer, and then CEL2 powders were added to the solution. The water evaporated during PVA dissolution was re-added in order to obtain the starting solid load (30 %wt.). The sponge blocks were soaked into the

glass slurry for 30 s and taken back for several times, followed by cycles of compression (20 kPa for 1 s) to reduce the sponge in thickness along the three spatial directions, in order to remove the exceeding slurry. The process replicates the structure of the starting polymeric foam and by optimising the number of infiltration/compression cycles, as described elsewhere [21], scaffolds with different degree of porosity can be successfully produced. Impregnated PU sponges subjected to different infiltration processes were stacked and underwent a thermal treatment obtaining glass-ceramic scaffolds with regions of different porosity.

Method D: scaffolds coupling a porous layer with a compact one were fabricated. The porous region was obtained with the sponge replication method whereas CEL2 powders were uniaxially pressed (127 MPa for 10 s) to realize the compact layer. The two layers were stacked together and thermally treated.

Method E: samples similar to those obtained with method D were produced. The sponge replication method was adopted to produce the porous scaffold; the compact layer was realized via glazing-like technique manually applying the CEL2 slurry with a spatula.

 Method F: the graded scaffolds were fabricated by stacking a PE-CEL2 green and an impregnated sponge and by thermally treat them.

Figure 1 depicts a schematic representation of the samples prepared according to the proposed methods. The thermal treatment was set at 1000 °C for 3 h (heating and cooling rate were 5 and 10 °C·min^{-1} respectively) for all methods in order to attain a good sintering degree of the scaffolds; PE and PU templates were completely removed at 500 and 600 °C respectively [20,19]. The differential thermal analysis (DTA), performed in a previous work [20], showed two crystallization temperatures (T_{X1} = 600 °C and T_{X2} = 800 °C) and thus, as the sintering temperature is higher than T_{X2}, the resulting scaffold material is glass-ceramic. The CEL2 melting temperature was found to be 1050 °C.

In addition bulk CEL2 samples were prepared as references to simulate the cortical bone. At this purpose, bars of CEL2 powders ("greens") were prepared via uniaxial pressing (127 MPa for 10 s) and then sintered at 1000 °C for 3 h, cut and polished using a 600 grit SiC paper to obtain cubic blocks (S-CEL2).

The features of all the series prepared in this work and their correspondence with human natural bone are summarized in table 1.

Scaffolds characterization

CEL2 was characterized by means of wide-angle ($10° < 2\theta < 70°$) X-ray diffraction analysis (XRD) using a X'Pert diffractometer (Bragg-Brentano camera geometry, Cu anode with Kα incident radiation). XRD analysis was also performed on the scaffold reduced into powders to detect the presence of crystalline phases after sintering.

Scaffolds morphology and microstructure were evaluated through scanning electron microscopy (SEM, Philips 525 M) to assess the pore size and distribution and to analyze the interface between the different layers forming the scaffold.

The whole porosity content (% vol.) of the scaffolds, including the contribution of both macropores and micropores, was assessed through geometrical weight-volume evaluations on five specimens for each series.

Specifically, the total porosity P (%vol.) was calculated as

$$P = \left(1 - \frac{w_s}{w_0}\right) \times 100 \,,$$

where w_s is the measured weight of the scaffold and w_0 the theoretical one calculated by multiplying the glass density ($\rho \approx 2.6$ g·cm^{-3}) and the sample volume.

The volumetric shrinkage S_V (%) of the scaffolds, due to the pore formers removal (PU template and/or PE particles) and to the CEL2 softening/sintering, was assessed for each series of samples as

$$S_V = \left(1 - \frac{V_s}{V_0}\right) \times 100,$$

where V_s is the scaffold volume and V_0 is the volume of the sample before the thermal treatment.

The scaffolds were carefully polished to obtain samples suitable for the mechanical tests. The strength of the scaffolds was evaluated through destructive compressive tests (MTS System Corp. machine, cross-head loading speed set at 1 mm·min^{-1}) performed on five specimens for each preparation method. The failure stress σ_f (MPa) was obtained as

$$\sigma_f = \frac{F_M}{A},$$

where F_M (N) is the maximum compressive load registered during the test and A (mm^2) is the cross-sectional area perpendicular to the load axis.

In addition *in vitro* bioactivity tests were carried out by soaking the scaffold in simulated body fluid (SBF), prepared according to Kokubo's protocol [30], that mimics the ion composition of human plasma. The samples were soaked for 7 days in PE bottles filled with 30 ml of SBF at 37 °C (human body temperature); the solution was replaced every 48 h to approximately simulate fluid circulation in human body. The pH value variations of the solution, induced by ion-exchange phenomena, were daily monitored (SBF reference value: pH = 7.40). The modifications of sample surface after soaking (formation of a HA layer) were investigated through SEM, EDS (Philips EDAX 9100) and XRD analysis.

RESULTS AND DISCUSSION

The PE particles used as pore formers for the scaffolds obtained via PE burn-off are depicted in figure 2(a). The PE grains are prism-shaped and ranged from 300 up to 600 μm.

Figure 2(b) shows the structure of the PU sponge used as polymeric template for CEL2 scaffolds prepared via the sponge replication method. The sponge exhibits a highly interconnected 3-D

network of macropores ranging within 200-1000 μm with a wall thickness of few tens of microns. As assessed through TG analysis (data not reported here), PE particles and the PU sponge were completely removed at 500 °C and 600 °C respectively, thus no scaffold contaminations was expected and actually occurred after the thermal treatment.

XRD analysis

Figure 3 shows the comparison between XRD patterns of as-molten CEL2 and of CEL2 scaffold reduced into powders. As it can be observed in figure 3(a), the broad halo confirms that the starting material was completely amorphous. The thermal treatment of sintering adopted to produce porous scaffolds (1000 °C for 3 h) induced the nucleation of two crystalline phases (fig. 3(b)) that were identified as combeite ($Na_4Ca_4(Si_6O_{18})$, JCPDF code 01-078-1649) and akemanite ($Ca_2Mg(Si_2O_7)$, JCPDF code 01-077-1149); therefore the resulting scaffolds are glass-ceramic. These data are consistent with the DTA results that assessed two crystallization temperatures T_{XX} [20].

Morphological investigations

Figure 4 shows the cross-section of a graded scaffold prepared with method A. The two regions of different porosity, *i.e.* 50 %vol. and 25 %vol. respectively can be seen. An excellent joining was reached between the two layers and no cracks or discontinuity can be seen at the interface. The pores, specifically in the most porous layer, are open and interconnected. More complex scaffolds with multiple layers of different porosity can be easily prepared, attaining a gradual transition in the pores content.

A sample prepared with method B, *i.e.* able to combine a porous layer, mimicking the cancellous bone, with another one similar to cortical bone, is shown in figure 5. As it can be observed, any defects is present at the interface between the cortical and the cancellous structure and a diffuse

microporosity is present in the compact layer in good accordance with the cortical bone feature that contains ~5 % vol. of porosity. A microporous texture is favourable for proteins and cells adhesion and thus the proposed method is of interest.

Method C involved the joining between two regions with different porosity prepared via the sponge replication technique and figure 6 reports a polished cross section of this type of sample. The two impregnated sponge were successfully joined together without defects and no cracks at the interface are visible. The morphology of the scaffold produced with the sponge method was discussed in details in previous works [20-21] and is similar to cancellous bone. The difference in terms of pores content between the two layers can be observed and more specifically the upper region contains about 50 %vol. of pores and the other about 70 % vol..

 Methods D and E led to very similar results; in figure 7 (method E), a nice interface can be seen between the "cancellous" and the "cortical" region. Micropores are visible in the compact layer in good accordance with the cortical bone pore content and to the microporous texture feature already observed in method B samples. Due to the easiness of fabrication for method E, method D was not further investigated.

In figure 8 a cross-section of a scaffold prepared with method F is reported. In this case, at the interface the two layers are joined together but, as can be seen in figure 8(b), in some points, a discontinuity area was observed.

As shown in the presented micrographs, the interfaces in all the prepared graded scaffolds are not a source of weakness with the exception of sample F.

In fact, although the interface has a finite number of contact points due to the high pores content, the two layers join firmly together. In addition, a 3-D network of interconnected pores is ensured, also at the interface, for the totally porous graded scaffolds (methods A, C and F).

A promising application of the proposed graded scaffolds concerns graft fixation to patient bone. In fact the scaffold is usually anchored to the surrounding bone by means of metal pins or screws, but this technique is unfit for highly porous implants. Drilling the scaffold can fracture its trabeculae

damaging the graft quality and moreover, the screw could be unstable in its seat. A compact CEL2 layer coupled to a porous scaffold can be an effective support for orthopaedic screws, as qualitatively shown in figure 9. At this purpose, the most interesting samples for future studies and applications are those prepared with methods B and E.

Finally, it should be underlined that the thickness of the compact layer can be adjusted after the scaffold sintering by polishing the sample, using for example a grit SiC paper. In fact, at the ends of the long bones the cortical bone thickness is within 1-3 mm [2], and this range should be considered as a reference for scaffolds preparation to obtain results consistent with natural bone. Aiming this, the samples prepared for pores analysis and mechanical tests were carefully polished to reach a compact layer final thickness of about 2.0 mm.

Pores analysis

The porosity of the prepared samples was assessed by means of geometrical weight-volume measurements carried out on five specimens for each series. Table 2 reports the so calculated porosity values that, including the contribution both of macropores and micropores, refer to the whole pores content of the samples. It should be noticed that the porous layers of methods C and E were prepared with a pores content above 50 %vol., as required for a scaffold mimicking the cancellous bone [22].

The volumetric shrinkage of the samples is also reported in table 2 and it is a very important parameter as it allows to tailor the final graded scaffold in terms of size and shape in order to fabricate "custom-made" grafts able to satisfy the requirements of specific clinical cases.

A low standard deviation was found both for the porosity and for the volumetric shrinkage of the samples, assessing a good reproducibility of the adopted preparation methods.

Mechanical tests

Five samples for each series underwent compressive mechanical test; the resulting failure stresses are reported in table 3. All the samples exhibit a mechanical strength comparable to human cancellous bone, taking into account that the graded structures prepared by methods B, D and E, mimic the cancellous-cortical bone system. The scaffolds prepared with the burn-off method showed higher structural strength: 11.5 MPa in the multi-layer porous form and 18 MPa in the "cancellous-cortical" system. The obtained values are due to the peculiar morphology of these scaffolds in which the pores are separated by dense regions without the presence of the trabecular structure observed for the samples produced with the replication method. The higher mechanical strength is thus negatively balanced by a morphology different than the one found in cancellous bone and by a lower interconnection degree of the pores.

Examples of stress-strain curves corresponding to the proposed preparation methods are reported in figure 10. As foreseen, all the samples show a failure mode typical for brittle ceramics, *i.e.* the catastrophic failure after the maximum stress. The graphs corresponding to methods A, B, C and E (figures 10(a)–(d)) exhibit a similar trend. Specifically, the curves show a first peak with a positive slope; afterwards an apparent stress drop followed by a saw-toothed profile occurs. The stress drop is due to the cracking onset of scaffold thin struts; then, the progressive crushing of the trabeculae gives the jagged trend of the curve. This behaviour, peculiar to ceramic foams and cellular glasses, is known as "pop-in behaviour" [30]. The second peak corresponds to thick trabeculae cracking and after reaching the maximum stress the curves exhibit a negative slope. In figures 10(a)–(b), after this drop the stress values further increase because the densification of the fractured scaffold, reduced into powders, occurs [31].

It should be noticed that the presence of a compact layer coupled to a porous one (methods B and E, figures 10(b) and 10(d) respectively) induces no substantial modifications in the stress-strain curve profile if compared to completely porous scaffolds (methods A and C, figures 10(a) and 10(c)

respectively), but in the former case the stress data shift to higher values particularly for the samples produced with the replication method. In fact in this case, the presence of a cortical layer allowed to obtain a cancellous-cortical system of remarkable strength (almost 10 MPa). Samples E are of great interest as they combine mechanical soundness and a morphology similar to the cancellous-cortical bone.

The curve corresponding to method F can be divided into two regions, as depicted in figure 10(e). Part I corresponds to the progressive cracking of the layer prepared via sponge replication, *i.e.* the low-strength layer of the graded scaffold and part II can be attributed to the crushing of the layer obtained via PE burn-off, *i.e.* the high-strength layer. Therefore, a 4-steps failure behaviour occurs for the scaffolds prepared with method F: cracking of (i) the thin trabeculae and (ii) the thick trabeculae in the low-strength layer followed by the crushing of (iii) the thin trabeculae and (iv) the thick trabeculae in the high-strength layer.

Figure 10(f) reports the curve for a massive sample (S-CEL2). Because of the porosity was lower than 5 %vol., the graph exhibits a positive slope and a unique peak corresponding to sample fracturing, as expected from a bulk ceramic.

In vitro **bioactivity tests**

As an example of *in vitro* bioactivity investigation, figure 11(a) shows the modifications induced on a C method sample after soaking for 7 days in SBF. A compact and homogeneous layer of a newly formed phase, constituted by globe-shaped agglomerates, is clearly visible. The compositional analysis, reported in figure 11(b), showed a molar ratio Ca/P ≈ 1.69, close to natural hydroxyapatite (HA) value (Ca/P ≈ 1.67). The presence of silver (Ag) peaks in EDS pattern is due to the metal coating necessary for the sample analysis. The scaffold was further investigated by means of XRD analysis (figure 11(c)), that confirmed the presence of HA (JCPDF code 01-082-1943), whereas the peaks corresponding to the scaffold crystalline phases are not visible demonstrating the continuity

and thickness of the newly formed HA layer. The main peak ($2\theta \approx 32°$) is broad due to the microcrystalline nature of HA nucleated on sample surface.

The presence of a HA layer on scaffold walls is a crucial feature able to promote the implant colonization by bone cells as it was demonstrated that osteoblasts attach and spread preferably on HA crystals [19].

Finally, the variations of pH value were quite moderate in the solution: an increase from 7.40 up to 8.0 was found after 24 h of soaking and after 7 days a value of 7.55 was detected.

CONCLUSIONS

In this work, the feasibility of graded glass-ceramic scaffolds for bone grafting was tested by using different methods of fabrication. Specifically, the sponge replication, the PE burn-off and the glazing technique were adopted for samples preparation. Scaffolds able to mimic the porosity gradients of cancellous bone and to reproduce the trabecular/cortical bone system were successfully produced. The obtained samples exhibited structure, morphology and mechanical strength comparable either to natural cancellous bone or to cancellous-cortical bone system, depending on the method used for preparation. In addition, the scaffolds were characterized by excellent bioactive properties.

The proposed methods of fabrication are efficient and reproducible. Many potential biomedical applications could be developed by using graded glass-ceramic scaffolds, such as grafts for the substitution of both small and extensive bone portions, also in load-bearing bone segment. In particular, the ease of processing will make it possible to fabricate a wide range of complex shapes according to specific aims of bone surgery. The presence of an outer compact layer can be useful also for fixing a synthetic grafts with screws avoiding the damage of its trabecular structure.

ACKNOWLEDGEMENTS

REFERENCES

1. Bonfield, W. (1984). Elasticity and Viscoelasticity of Cortical Bone. In: Natural and Living Biomaterials, ed. by Hastings, G.W. and Ducheyne, P., CRC Press, Boca Raton, Florida, p. 43.

2. Van Audekercke, R. and Martens, M. (1984). Mechanical Properties of Cancellous Bone. In: Natural and Living Biomaterials, ed. by Hastings, G.W. and Ducheyne, P., CRC Press, Boca Raton, Florida, p. 89.

3. Cowin, S.C. (1984). The mechanical properties of cancellous bone. In: Bone Mechanics, ed. by Cowin, S.C., CRC Press, Boca Raton, Florida, p. 130.

4. Thompson, J.D and Hench, L.L. (1998). Mechanical properties of bioactive glasses, glass-ceramics and composites, *J. Eng. in Med.*, **212**: 127–136.

5. Goldstein, S.A. (1987). The mechanical properties of trabecular bone: dependence on anatomic location and function, *J. Biomech.*, **20**: 1055–1061.

6. Schlickewei, W. and Schlickewei, S. (2007). The use of bone substitutes in the treatment of bone defects – The clinical view and history, *Macromol. Symp.*, **253**: 10–23.

7. Hoop, S.G., Dahners, L.G. and Gilbert, J.A. (1989). Study of the mechanical strength of long bone defects treated with various bone autograft substitutes: an experimental investigation in the rabbit, *J. Orthop. Res.*, **7**: 579–584.

8. Ries, M.D., Gomez, M.A., Eckhoff, D.G., Lewis, D.A., Brodie, M.R. and Wiedel, J.D. (1994). An in vitro study of proximal femoral allograft strains in revision hip arthroplasty, *Med. Eng. Phys.*, **16**: 292–296.

9. Jones, J. and Hench, L.L. (2003). Regeneration of trabecular bone using porous ceramics, *Curr. Opin. Solid State Mater. Sci.*, **7**: 301–307.

10. Ozawa, N., Negami, S., Odaka, T., Morii, T. and Koshino, T. (1989). Histological observations on tissue reaction of the rat calcaneal tendon to sintered hydroxyapatite, *J. Mater. Sci. Lett.*, **8**: 869–871.

11. LeGeros, R.Z. (1993). Biodegradation and bioresorption of calcium phosphate ceramics, *Clin. Mater.*, **14**: 65–88.

12. LeGeros, R.Z., Lin, S., Rohanizadeh, R., Mijares, D. and LeGeros, J.P. (2003). Biphasic calcium phosphate bioceramics: preparation, properties and applications, *J. Mater. Sci.: Mater. Med.*, **14**: 201–209.

13. Thomson, R.C., Yaszemski, M.J., Powers, J.M. and Mikos, A.G. (1998). Hydroxyapatite fiber reinforced poly(α-hydroxy ester) foams for bone regeneration, *Biomaterials*, **19**: 1935–1943.

14. Xigeng, M., Tan, D.M., Jian, L., Yin, X. and Crawford, R. (2008). Mechanical and biological properties of hydroxyapatite/tricalcium phosphate scaffolds coated with poly(lactic-co-glycolic acid), *Acta Biomater.*, **4**: 638–645.

15. Hench, L.L. and Anderson, O. (1993). Bioactive glasses. In: An introduction to bioceramics, ed. by Hench, L.L. and Wilson, J., World Scientific, Singapore, p. 41.

16. Hench, L.L. (1998). Bioactive materials: the potential for tissue regeneration, *J. Mater. Biomed. Res.*, **41**: 511–518.

17. Jones, J.R., Ehrenfried, L.M. and Hench, L.L. (2006). Optimising bioactive glass scaffolds for bone tissue engineering, *Biomaterials*, **27**: 964–973.

18. Vitale-Brovarone, C., Verné, E. and Appendino, P. (2006). Macroporous bioactive glass-ceramic scaffolds for tissue engineering, *J. Mater. Sci.: Mater. Med.*, **17**: 1069–1078.

19. Vitale-Brovarone, C., Verné, E., Robiglio, L., Appendino, P., Bassi, F., Martinasso, G., Muzio, G. and Canuto, R. (2007). Development of glass-ceramic scaffolds for bone tissue engineering: Characterisation, proliferation of human osteoblasts and nodule formation, *Acta Biomater.*, **3**: 199–208.

20. Vitale-Brovarone, C., Verné, E., Robiglio, L., Martinasso, G., Canuto, R.A. and Muzio, G. (2008). Biocompatible glass-ceramic materials for bone substitution, *J. Mater. Sci.: Mater. Med.*, **19**: 471–478.

21. Vitale-Brovarone, C., Baino, F. and Verné, E. (2009). High strength bioactive glass-ceramic scaffolds for bone regeneration, *J. Mater. Sci.: Mater. Med.*, **20**: 643–653.

22. Adachi, T., Osako, Y., Tanaka, M., Hojo, M. and Hollister, S.J. (2006). Framework for optimal design of porous scaffold microstructure by computational simulation of bone regeneration, *Biomaterials*, **27**: 3964–3972.

23. Livingston, T., Ducheyne, P. and Garino, J. (2002). In vivo evaluation of a bioactive scaffold for bone tissue engineering, *J. Biomed. Mater. Res.*, **62**: 1–13.

24. De Aza, P.N., Luklinska, Z.B., Santos, C., Guitian, F. and De Aza, S. (2003). Mechanism of bone-like formation on a bioactive implant in vivo, *Biomaterials*, **24**: 1437–1445.

25. Schwarts, Z. and Boyan, B.D. (1994). Characterization of microrough bioactive glasses: surface reactions and osteoblast responses, *J. Cell. Biochem.*, **56**: 340–347.

26. Lyckfeldt, O. and Ferreira, J.M. (1998). Processing of porous ceramics by starch consolidation, *J. Eur. Ceramic Soc.*, **18**: 131–140.

27. Vitale-Brovarone, C., Di Nunzio, S., Bretcanu, O. and Verné, E. (2004). Macroporous glass-ceramics materials with bioactive properties, *J. Mater. Sci: Mater. Med.*, 15: 209–217.

28. Tampieri, A., Celotti, G., Sprio, S., Delcogliano, A. and Franzese, S. (2001). Porosity-graded hydroxyapatite ceramics to replace natural bone, *Biomaterials*, **22**: 1365–1370.

29. Hsu, Y.H., Turner, I.G. and Miles, A.W. (2008). Fabrication of porous bioceramics with porosity gradients similar to the bimodal structure of cortical and cancellous bone, *J. Mater. Sci.: Mater. Med.*, **18**: 2251–2256.

30. Kokubo, T. and Takadama, H. (2006). How useful is SBF in predicting in vivo bone bioactivity?, *Biomaterials*, **27**: 2907–2915.

31. Gibson, L.J. and Ashby, M.F. (1999). Cellular solids: structure and properties, 2nd Ed. Oxford, Pergamon, p. 117.

Figure

Figure 1. Features of the proposed methods for graded glass-ceramic scaffolds preparation.

Method A

Method B

Method C

Method D

Method E

Method F
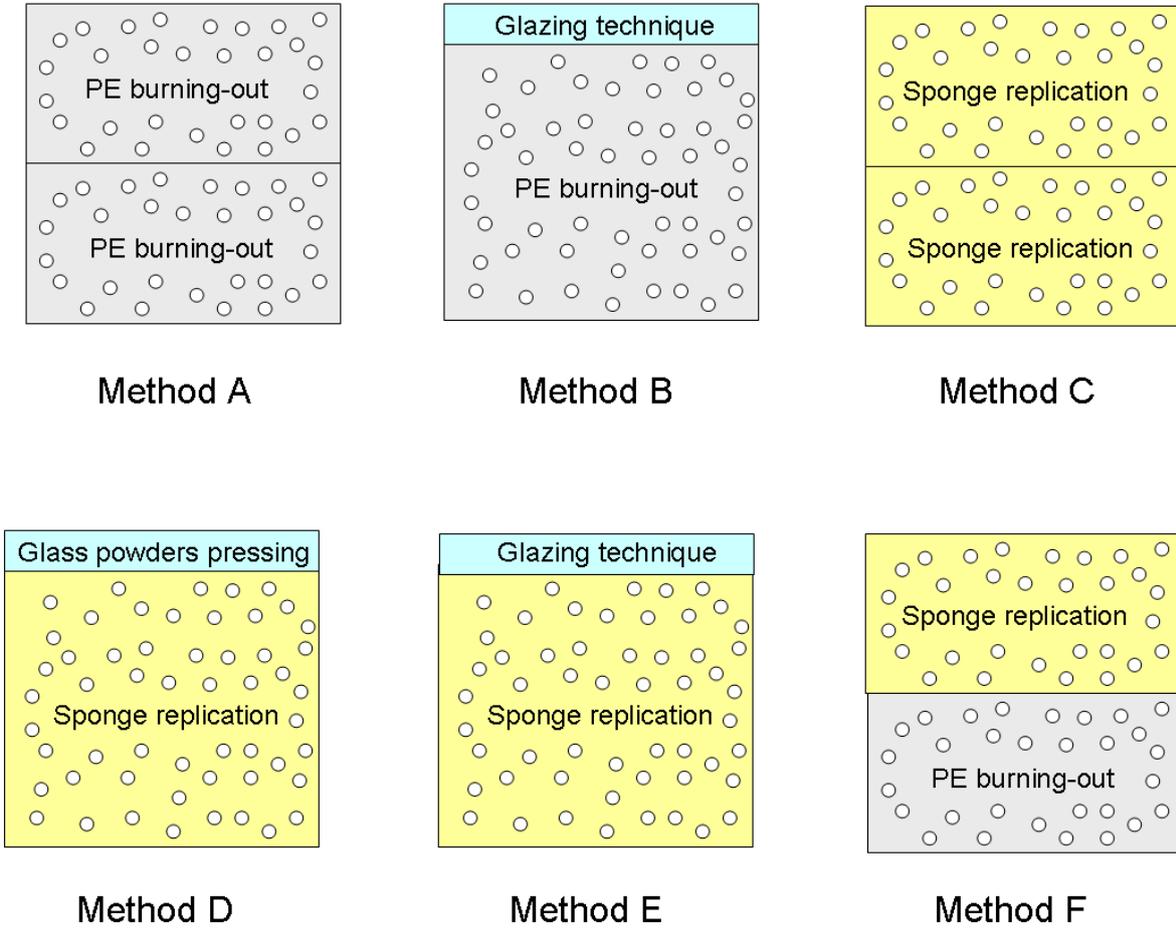
Figure 2. Polymeric templates used for scaffolds preparation: (a) polyethylene particles and (b) polyurethane sponge.
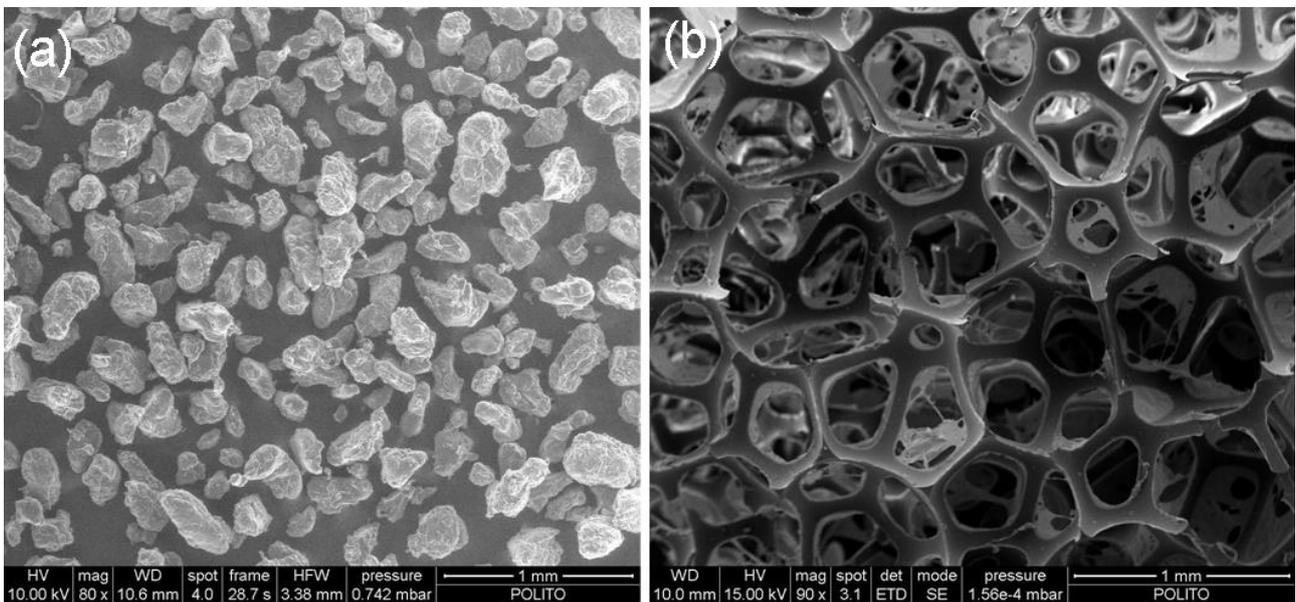
Figure 3. Diffraction spectra of (a) as-poured CEL2 and of (b) CEL2 scaffold obtained after sintering (1000 °C for 3 h).
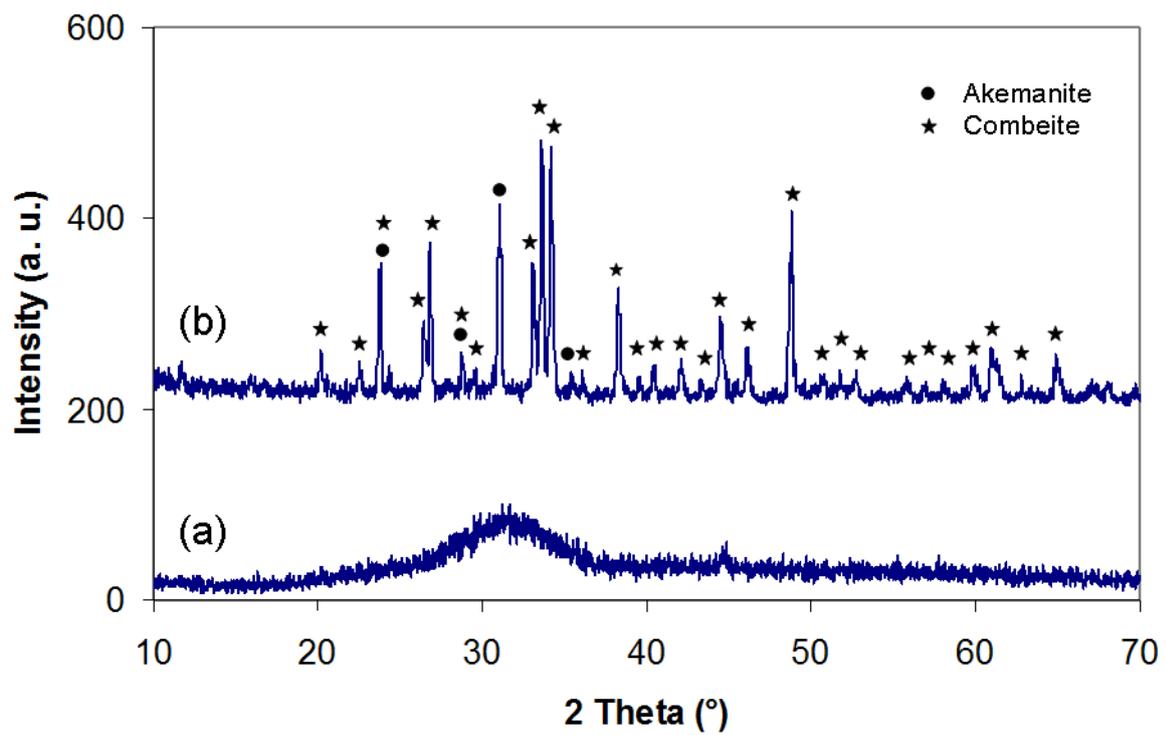
Figure 4. Cross-section of a double porous layered scaffold (50 %vol.-25 %vol.) prepared with method A.

HV	mag	WD	spot	frame	HFW	pressure		3 mm
15.00 kV	28 x	20.6 mm	4.0	28.4 s	9.75 mm	0.599 mbar		Inspect
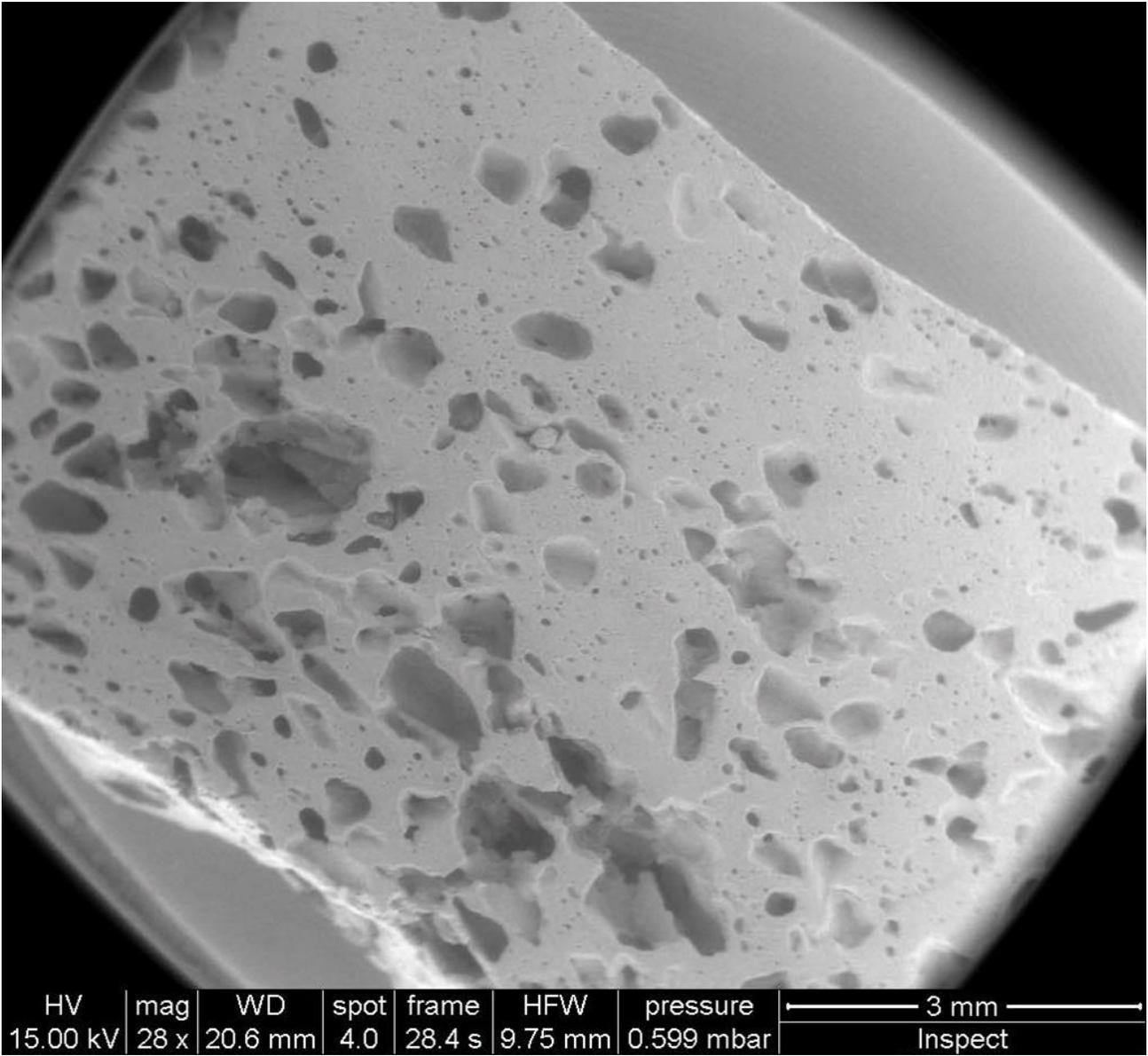
Figure 5. Micrograph of a graded scaffold obtained via method B.
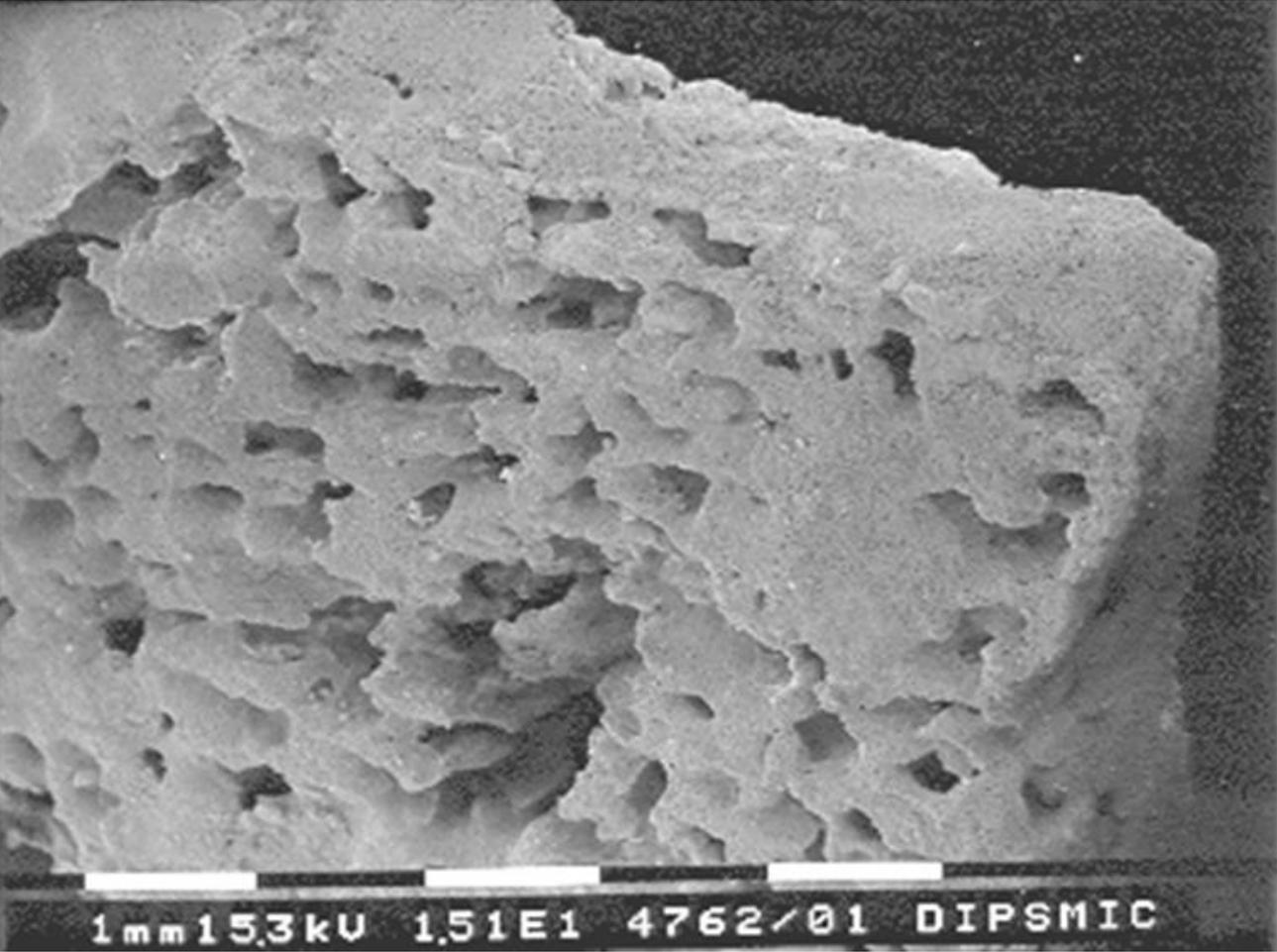
Figure 6. Scaffold fabricated through method C.
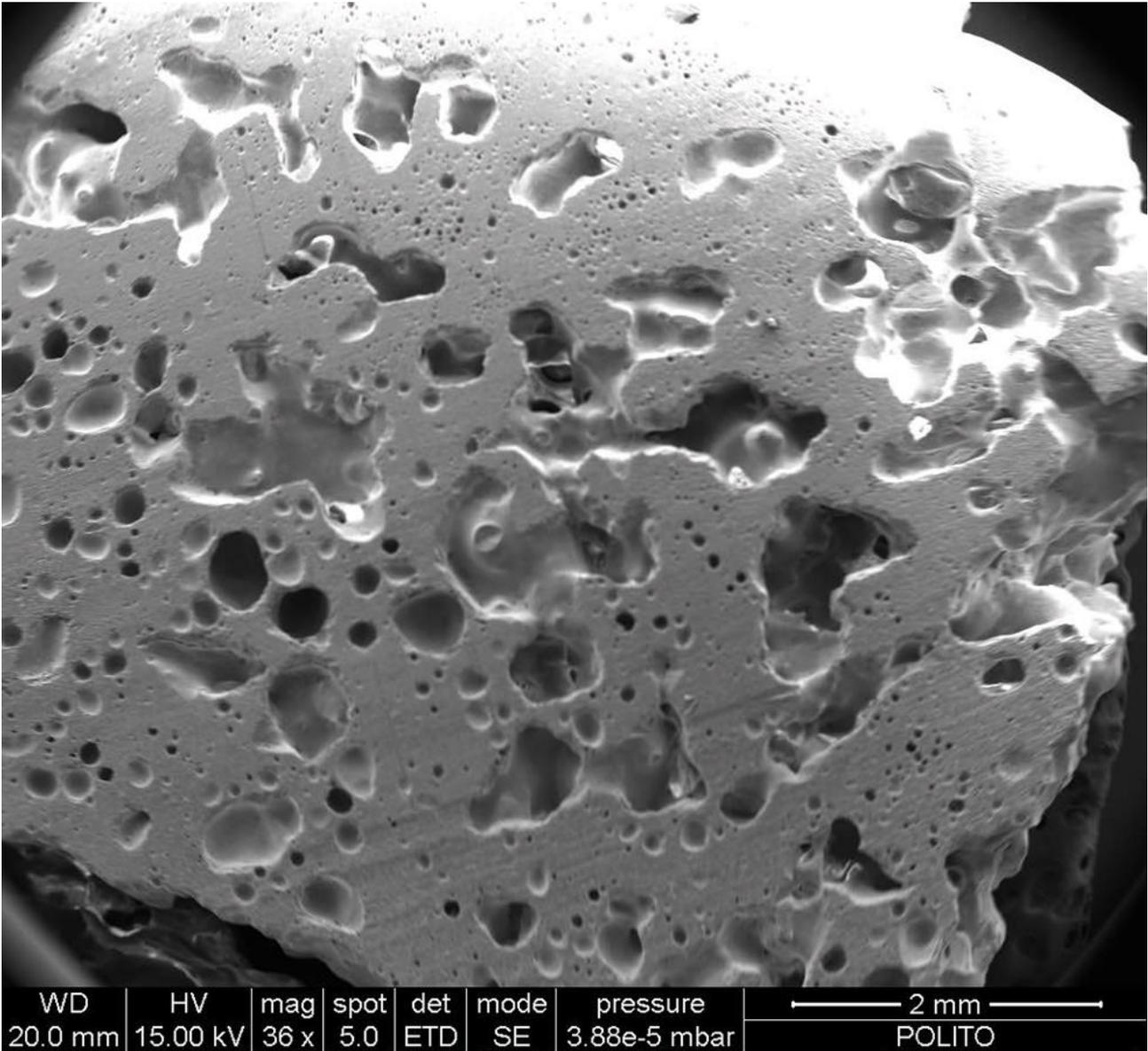
Figure 7. Micrographs of the porous/compact layer interface, at different magnifications, of a scaffold fabricated with method E.
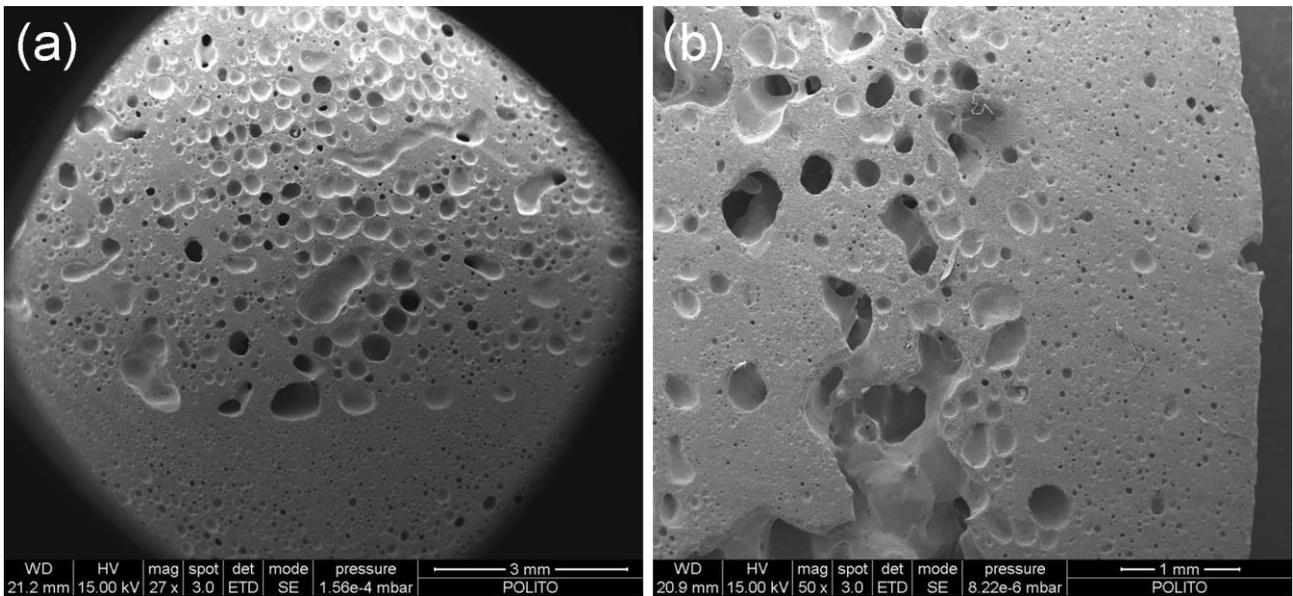

Figure 8. Interface between porous and compact layer in a graded scaffold (method F) at different magnifications.
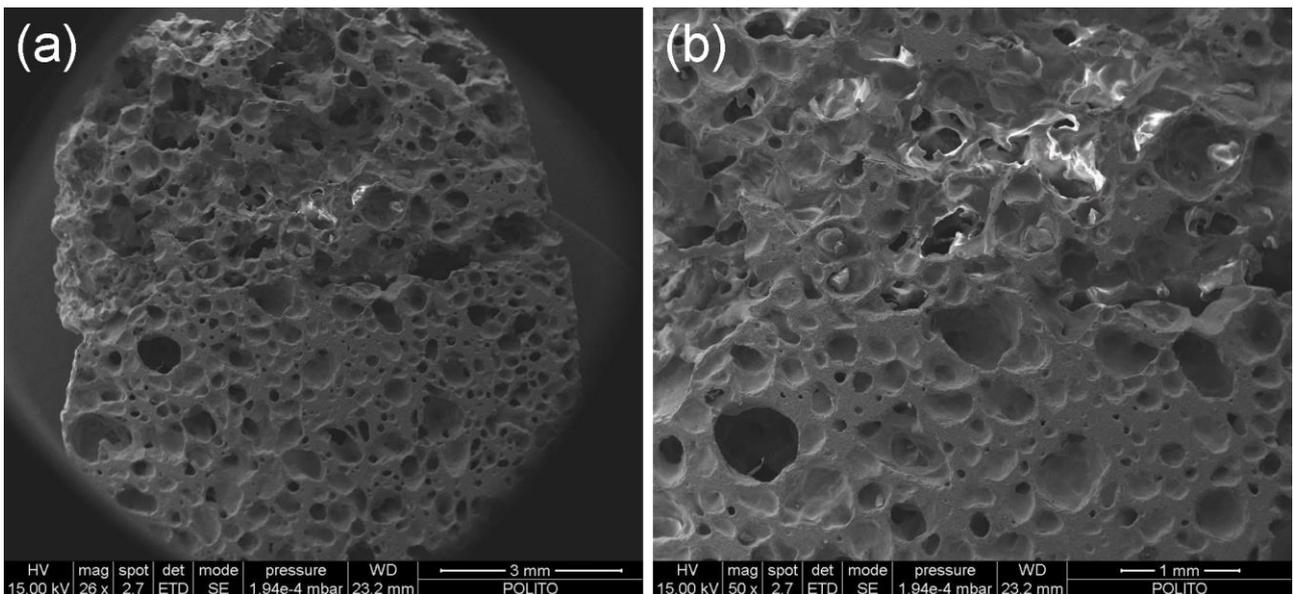
Figure 9. Application of graded scaffolds: (a) successful drilling of the graft and (b) insertion of a metal screw.
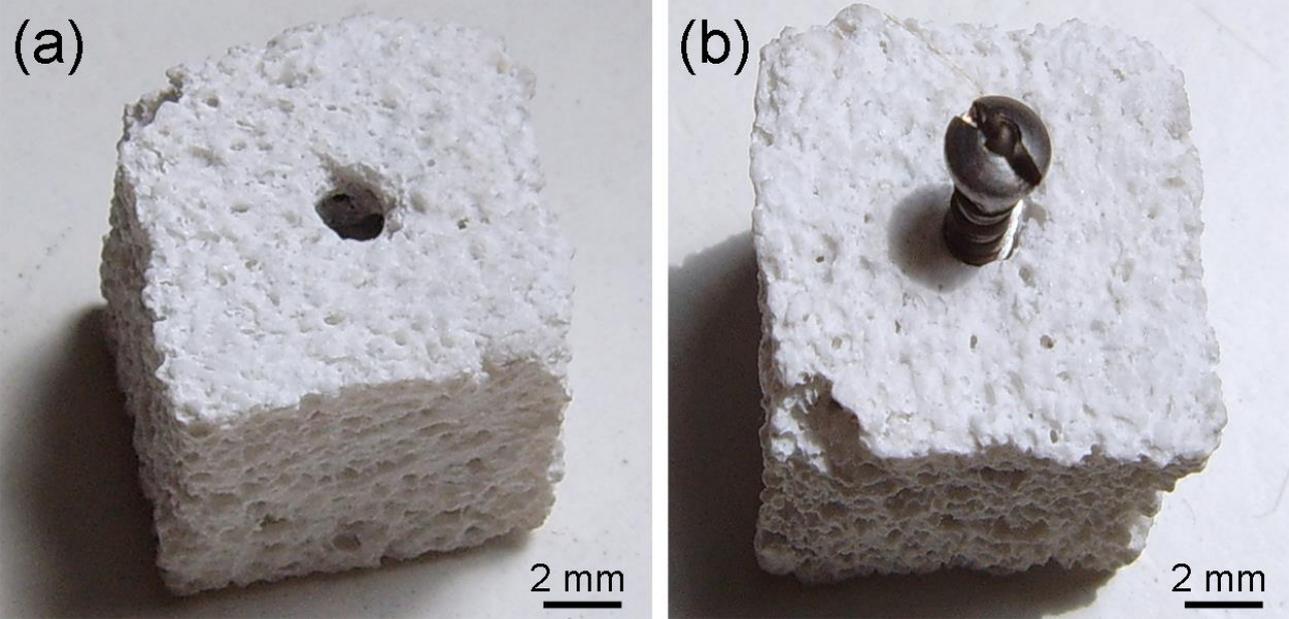
Figure 10. Examples of typical stress-strain curves for (a) method A, (b) method B, (c) method C, (d) method E, (e) method F and (f) S-CEL2 sample.
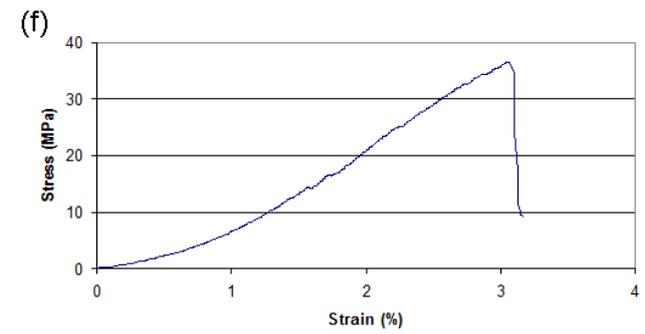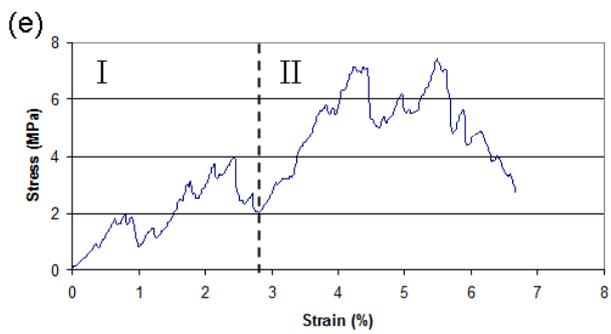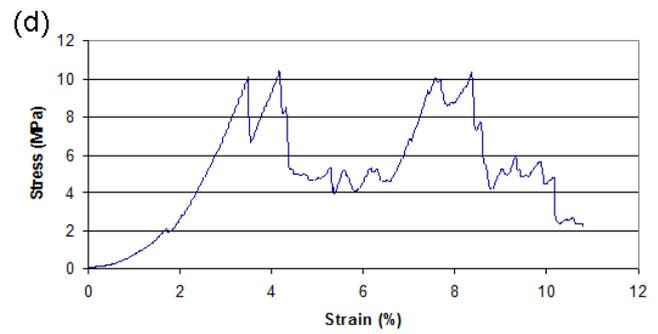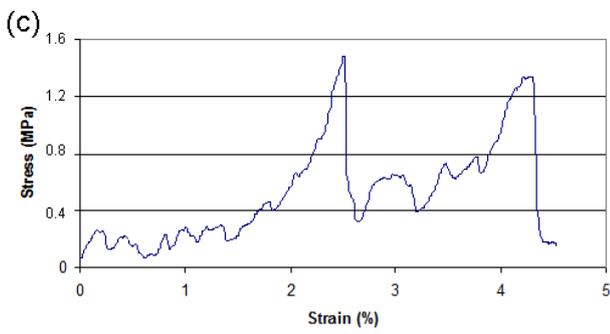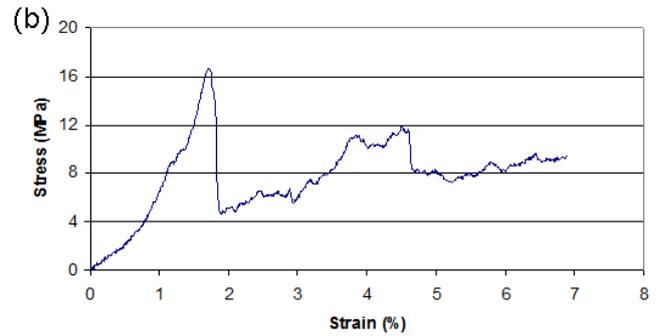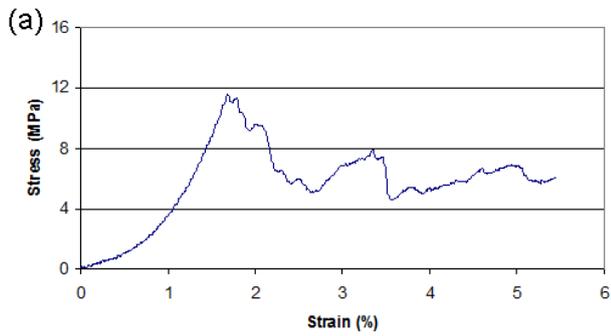
Figure 11. *In vitro* bioactivity test after 7 days of soaking in SBF: (a) newly formed HA layer on scaffold surface, (b) EDS analysis and (c) diffraction pattern.
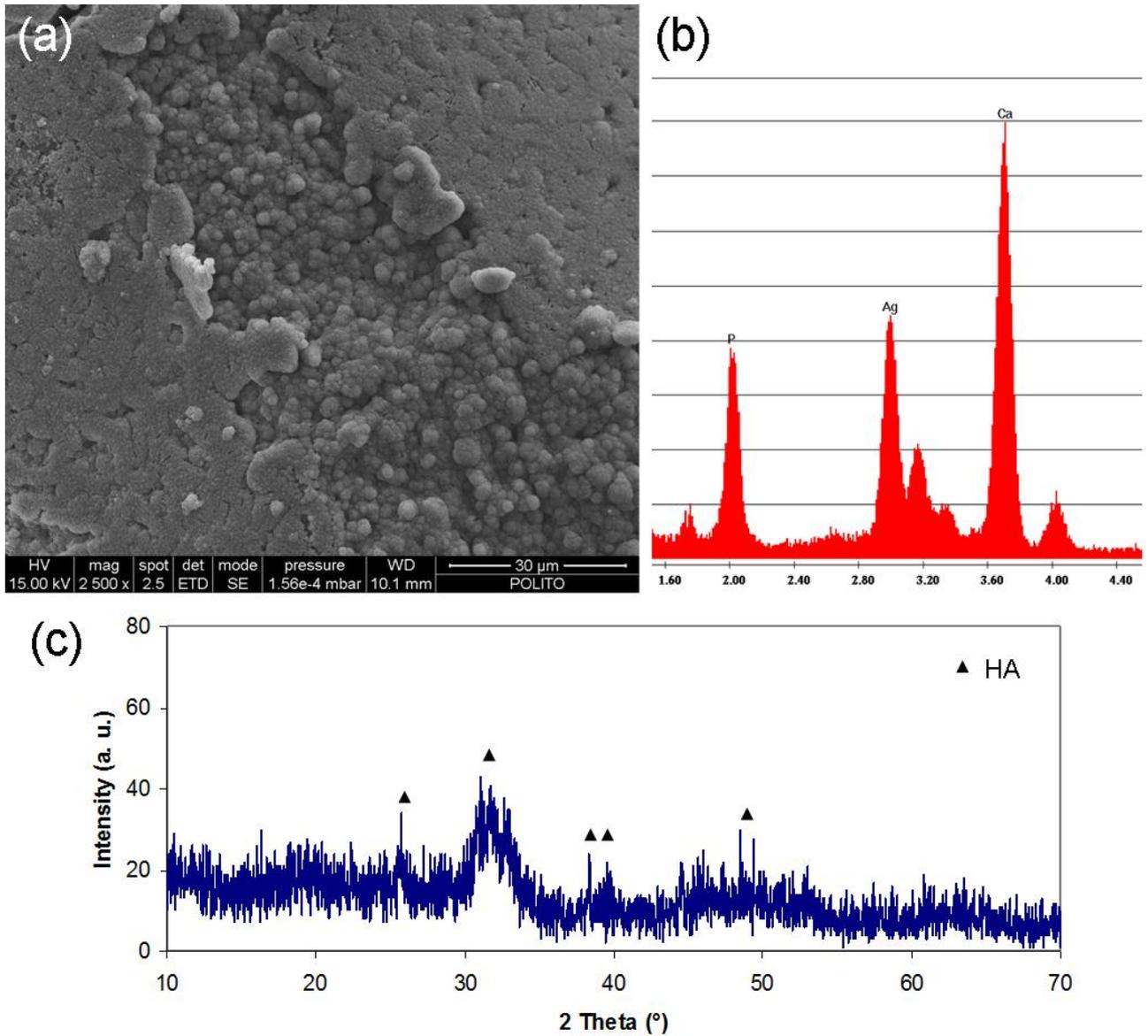
Tables

Table 1 Sample preparation methods.

Preparation method	Preparation details	Scaffold structure	Correspondence with human bone
A	PE burn-off	Multi-layer structure	Cancellous bone
B	PE burn-off + glazing technique	Porous layer + compact layer	Cancellous/cortical bone system
C	Sponge replication	Porous double layer	Cancellous bone
D	Sponge replication + glass powders pressing	Porous layer + compact layer	Cancellous/cortical bone system
E	Sponge replication + glazing technique	Porous layer + compact layer	Cancellous/cortical bone system
F	Sponge replication + PE burn-off	Porous double layer	Cancellous bone
S-CEL2	Sintering of glass powder compacts	Bulk	Cortical bone

Table 2 Porosity content (via density measurements) and volumetric shrinkage of the samples.

Method	P (% vol.)	S_V (%)
A	27.6 ± 0.6	56.3 ± 3.2
B	29.3 ± 1.2	40.5 ± 3.4
C	64.6 ± 3.0	63.0 ± 4.3
E	53.0 ± 3.9	58.5 ± 4.5
F	47.3 ± 4.7	49.5 ± 3.8

Table 3 Compressive strength of the samples.

Method	σ_f (MPa)
A	11.5 ± 2.9
B	18.0 ± 3.0
C	1.9 ± 0.2
E	9.7 ± 2.6
F	6.3 ± 1.5
S-CEL2	32.5 ± 6.5